Engineered protein degradation of farnesyl pyrophosphate synthase is an effective regulatory mechanism to increase monoterpene production in Saccharomyces cerevisiae

Peng, Bingyin; Nielsen, Lars Keld; Kampranis, Sotirios C; Vickers, Claudia E

Published in:
Metabolic Engineering

Link to article, DOI:
10.1016/j.ymben.2018.02.005

Publication date:
2018

Document Version
Peer reviewed version

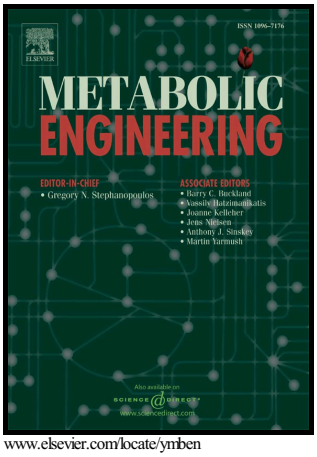

www.elsevier.com/locate/ymben

Engineered protein degradation of farnesyl pyrophosphate synthase is an effective regulatory mechanism to increase monoterpene production in *Saccharomyces cerevisiae*

Bingyin Peng, Lars K. Nielsen, Sotirios C. Kampranis, Claudia E. Vickers

PII: S1096-7176(17)30214-8
DOI: https://doi.org/10.1016/j.ymben.2018.02.005
Reference: YMBEN1344

To appear in: *Metabolic Engineering*

Received date: 29 June 2017
Revised date: 2 February 2018
Accepted date: 14 February 2018

Cite this article as: Bingyin Peng, Lars K. Nielsen, Sotirios C. Kampranis and Claudia E. Vickers, Engineered protein degradation of farnesyl pyrophosphate synthase is an effective regulatory mechanism to increase monoterpene production in *Saccharomyces cerevisiae*, *Metabolic Engineering,* https://doi.org/10.1016/j.ymben.2018.02.005

Engineered protein degradation of farnesyl pyrophosphate synthase is an effective regulatory mechanism to increase monoterpene production in *Saccharomyces cerevisiae*

Bingyin Peng; Australian Institute for Bioengineering and Nanotechnology (AIBN), the University of Queensland, St. Lucia, QLD 4072, Australia. b.peng@uq.edu.au

Lars K. Nielsen; Australian Institute for Bioengineering and Nanotechnology (AIBN), The University of Queensland, St. Lucia, QLD 4072, Australia; Novo Nordisk Foundation Center for Biosustainability, Technical University of Denmark, Kemitorvet, 2800 Kgs, Lyngby, Denmark. lars.nielsen@uq.edu.au

Sotirios C. Kampranis; Department of Plant and Environmental Sciences, University of Copenhagen, Thorvaldsensvej 40, 1871 Frederiksberg C, Denmark. soka@plen.ku.dk

Claudia E. Vickers; Australian Institute for Bioengineering and Nanotechnology (AIBN), The University of Queensland, St. Lucia, QLD 4072, Australia; corresponding author; CSIRO Future Science Platform in Synthetic Biology, Commonwealth Scientific and Industrial Research Organisation (CSIRO), Australia. c.vickers@uq.edu.au; **Corresponding author.**

Abstract

Monoterpene production in *Saccharomyces cerevisae* requires the introduction of heterologous monoterpene synthases (MTSs). The endogenous farnesyl pyrosphosphate synthase (FPPS; Erg20p) competes with MTSs for the precursor geranyl pyrophosphate (GPP), which limits the production of monoterpenes. *ERG20* is an essential gene that cannot be deleted and transcriptional down-regulation of *ERG20* has failed to improve monoterpene production. Here, we investigated an N-degron-dependent protein degradation strategy to down-regulate Erg20p activity. Degron tagging decreased GFP protein half-life drastically to 1 hour (degron K3K15) or 15 minutes (degrons KN113 and KN119). Degron tagging of *ERG20* was therefore paired with a sterol responsive promoter to ensure sufficient metabolic flux to essential downstream sterols despite the severe destabilisation effect of degron tagging. A dual monoterpene/sesquiterpene (linalool/nerolidol) synthase, *AcNES1*, was used as a reporter of intracellular GPP and FPP production. Transcription of the synthetic pathway was controlled by either constitutive or diauxie-inducible promoters. A combination of degron K3K15 and the *ERG1* promoter increased linalool titre by 27-fold to 11 mg L^{-1} in the strain with constitutive promoter constructs, and by 17-fold to 18 mg L^{-1} in the strain with diauxie-inducible promoter constructs. The sesquiterpene nerolidol remained the major product in both strains. The same strategies were applied to construct a limonene-producing strain, which produced 76 mg L^{-1} in batch cultivation. The FPPS regulation method developed here successfully redirected metabolic flux toward monoterpene production. Examination of growth defects in various strains suggested that the intracellular FPP concentration had a significant effect on growth rate. Further strategies are required to balance intracellular production of FPP and GPP so as to maximise monoterpene production without impacting on cellular growth.

Keywords: metabolic engineering, synthetic biology, flux competition/redirection, protein destabilization, prenyl pyrosphosphate synthase, monoterpene

1. Introduction

Metabolic engineering aims to enhance the productivity and the yield of the target metabolite through engineering metabolic and regulatory networks (Stephanopoulos and Vallino, 1991). Elimination or reduction of flux-competing reactions is commonly required to redirect metabolic flux toward the product of interest (Nielsen, 2011; Sabri et al., 2013). Gene deletion is used to remove reactions from the network; however, deletion in anabolic pathways can generate a lethal or auxotrophic phenotype. Lethality is obviously unhelpful, and addition of medium components to supplement for auxotrophies is cost-prohibitive in many industrial scenarios.

An alternative approach is down-regulation of the target reaction, commonly achieved at the transcriptional level. This has been well demonstrated for production of 15-carbon sesquiterpenes from the isoprenoid family of natural products in yeast (*Saccharomyces cerevisiae*). Isoprenoids are constructed from 5-, 10-, 15-carbon (etc.) precursors which are sequentially produced via condensation of the 5-carbon dimethylallyl pyrophosphase (DMAPP) and its isomer isopentenyl pyrophosphate (IPP; Figure 1) (Vickers et al., 2015a). Heterologous production of industrially useful isoprenoids in yeast suffers from competition by the native sterol pathway, which uses the 15-carbon precursor intermediate, farnesyl pyrophosphate (FPP). The flux-competing enzyme is squalene synthase (Erg9p), an endoplasmic reticulum-associated protein. Transcriptional down-regulation of *ERG9* by chromosomal promoter replacement (using *BTS1*, *HXT1*, or *CTR3* promoters) has been applied to decrease competition and redirect flux from sterols to heterologous sesquiterpenes (Paddon et al., 2013; Scalcinati et al., 2012; Xie et al., 2014). We recently demonstrated a protein degradation approach for successful down-regulation at this node using an endoplasmic reticulum associated protein degradation signal (Peng et al., 2017b), the first demonstration of engineered protein degradation for yeast metabolic engineering.

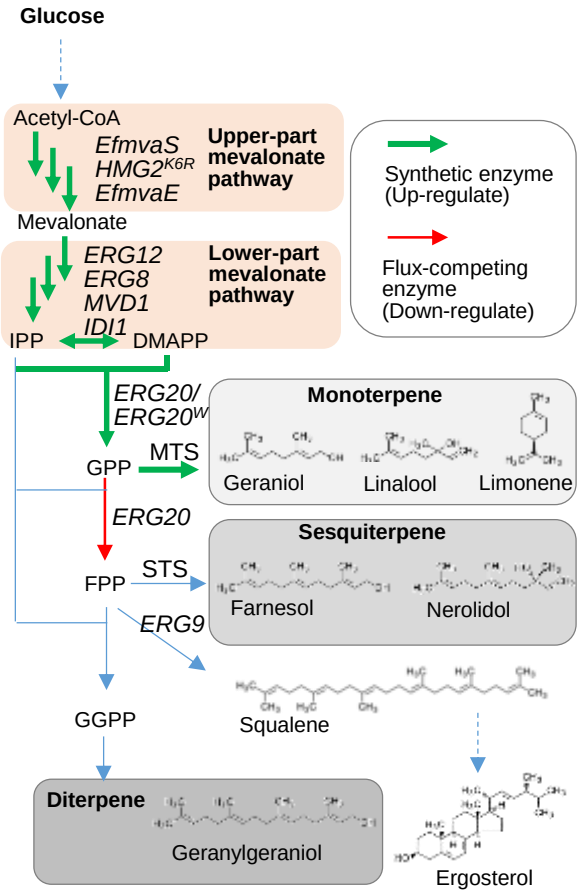

Figure 1. Metabolic pathways for the production of various terpenes. *EfmvaS*, *Enterococcus faecalis* hydroxymethylglutaryl-CoA (HMG-CoA) synthase; *EfmvaE*, *E. faecalis* acetoacetyl-CoA thiolase/HMG-CoA reductase; *HMG2*^{K6R}, HMG-CoA reductase 2 K6R mutant; *ERG12*, mevalonate kinase; *ERG8*, phosphomevalonate kinase; *MVD1*, mevalonate pyrophosphate decarboxylase; *IDI1*, isopentenyl diphosphate:dimethylallyl diphosphate isomerase; *ERG20*, farnesyl pyrophosphate synthase; *ERG20*^{W}, *ERG20* N127W mutant, geranyl pyrophosphate synthase; *ERG9*, squalene synthase; IPP, isopentenyl pyrophosphate; DMAPP, dimethylallyl pyrophosphate; GPP, geranyl pyrophosphate; FPP, farnesyl pyrophosphate; GGPP, geranylgeranyl pyrophosphate; MTS, monoterpene synthase; STS, sesquiterpene synthase.

There is significant interest in the industrial production of monoterpenes (10-carbon terpenoids) using yeast. Monoterpenes have attractive floral scents and useful biological activities (Zebec et al., 2016). They can also provide the light fraction for alternative kerosene jet-fuels (Brennan et al., 2012; Vickers et al., 2014). Monoterpenes are synthesized from the 10-carbon precursor geranyl pyrophosphate (GPP). However, in *S. cerevisiae*, GPP and FPP are synthesized by a bi-functional enzyme, farnesyl pyrophosphate synthase (FPPS; Erg20p), which converts DMAPP and IPP into GPP and adds another IPP to produce FPP (**Figure 1**) (Anderson et al., 1989; Parks et al., 1995). GPP is not normally released by FPPS and this limits GPP availability for monoterpene production.

Previously, enzymes from the mevalonate (MVA) pathway were over-expressed to increase precursor flux for terpene synthesis (Figure 1) (Peng et al., 2017a; Peng et al., 2017b; Vickers et al., 2017). A dedicated GPP synthase has been used to increase the GPP pool for monoterpene production (Alonso-Gutierrez et al., 2013; Amiri et al., 2016; Cao et al., 2016;

Liu et al., 2016; Rico et al., 2010; Sarria et al., 2014; Willrodt et al., 2014; Zhang et al., 2014). However, yields were low compared to production of sesquiterpenes in a similar system, suggesting that the native Erg20p competes effectively with the monoterpene synthase for GPP. *ERG20* is essential for anabolic metabolism of downstream essential cellular components including sterols, ubiquinone, and protein prenylation (Casey, 1992; Dickinson and Schweizer, 2004; Paltauf et al., 1992); deletion of *ERG20* is lethal (Anderson et al., 1989; Giaever et al., 2002). Down-regulation strategies have therefore been applied. Deletion of one allele in a diploid strain (*ERG20*/erg20) improved sabinene production compared to a haploid (*ERG20*) strain (Ignea et al., 2013). However, the transcriptional down-regulation approach that was successfully applied to *ERG9* for C15 production was unsuccessful when applied to down-regulate *ERG20* for monoterpene geraniol production (Zhao et al., 2016; Zhao et al., 2017). It appears that classical promoter-mediated transcriptional level control is ineffective for metabolic engineering at the Erg20p node.

In *S. cerevisiae*, ergosterol synthetic (ERG) enzymes are regulated both transcriptionally and through protein turnover mechanisms (Christiano et al., 2014). At the transcriptional level, *ERG* genes are regulated by sterol regulatory transcription factors including Upc2p (Vik and Rine, 2001; Yang et al., 2015). When ergosterol levels are high, ergosterol binds to the Upc2p carboxyl-terminal domain, preventing activity; when ergosterol is low, Upc2p is unbound and activates *ERG* gene transcription (Yang et al., 2015). This mechanism provides the basis for an exploitable feedback-control circuit that responds by increasing transcription in conditions of insufficient ergosterol. At the protein level, endoplasmic-reticulum-associated protein degradation (ERAD) modulates protein turnover of ER-associated ERG enzymes (Christiano et al., 2014; Foresti et al., 2013). Squalene epoxidase (*ERG1*) illustrates this multi-level regulation: *ERG1* is upregulated by Upc2p in response to low ergosterol (Servouse and Karst, 1986; Vik and Rine, 2001), while Erg1p is degraded through the ERAD pathway resulting in a short protein half-life (Foresti et al., 2013). We have previously exploited the ERAD mechanism to regulate Erg9p, resulting in flux redirection from squalene accumulation to sesquiterpene production (Peng et al., 2017b). In the current study, we aimed to improve monoterpene production by elevating the GPP pool. To achieve this, we developed an alternative protein degradation mechanism to downregulate the cytoplasmic FPP synthase and coupled it with an ergosterol responsive transcription modulator circuit, with the aim of producing high titres of monoterpenes while ensuring sufficient flux to sterols and avoid growth defects.

2. Materials and Methods

2.1 Plasmid and strain construction

Plasmids used in this work are listed in **Table 1** and strains are listed in **Table 2**. Primers used in polymerase chain reaction (PCR) and PCR performed in this work are listed in **Appendix 1: Table S1**. Plasmid construction processes are listed in **Appendix 1: Table S2**.

The *Swa*I-digested plasmids pILGF6, pILGF7 and pILGF8 were transformed separately into CEN.PK113-5D to generate GF6, GF7 and GF8.

Plasmid	Features	Addgene#	Reference
pILGFPE9	pILGFP3: P_{TEF1}-*yEGFP*	83545	(Peng et al., 2015)
pILGFPF6	pILGFP3: P_{TEF1}-*UBI4-Degron(F:K3K15)-yEGFP*	-	This work
pILGFPF7	pILGFP3: P_{TEF1}-*UBI4-Degron(F:KN119)-yEGFP*	-	This work
pILGFPF8	pILGFP3: P_{TEF1}-*UBI4-Degron(F:KN113)-yEGFP*	-	This work
pRS423	*E.coli/S. cerevisiae* shuttle plasmid; 2μ, *HIS3*	-	(Christianson et al., 1992)
pRS424	*E.coli/S. cerevisiae* shuttle plasmid; 2μ, *TRP1*	-	(Christianson et al., 1992)
pRS425	*E.coli/S. cerevisiae* shuttle plasmid; 2μ, *LEU2*	-	(Christianson et al., 1992)
pPMVAu8	pRS423: P_{RPL4A}>*EfmvaS*>T_{EFM1}-P_{RPL15A}>*EfmvaE* >T_{EBS1}	98297	(Peng et al., 2017b)
pPMVAd3	pRS424: P_{RPL8B}>*ERG12*>T_{NAT5}-P_{SSB1}>*ERG8*>T_{IDP1}-P_{RPL3}>*MVD1*>T_{PRM9}-P_{YEF3}>*IDI1*>T_{RPL15A}	98298	(Peng et al., 2017b)
pPMVAd40R	pRS424: *ERG9*$^{C\text{-}terminal}$-T_{URA3}- P_{GAL7}>*MVD1*>T_{PRM9}-P_{GAL2}>-*ERG12*>T_{NAT5}-T_{IDP1}<*ERG8*<P_{GAL10}-P_{GAL1}-*IDI1*-T_{RPL15A}-*loxP-ble-loxP*-T_{ERG9}	98309	This work
pPMVAd41	pRS424: *ERG9*$^{C\text{-}terminal}$-*CLN2*^{PEST}-T_{URA3}-P_{GAL7}>*MVD1*>T_{PRM9}-P_{GAL2}>-*ERG12*>T_{NAT5}-T_{IDP1}<*ERG8*<P_{GAL10}-P_{GAL1}-*IDI1*-T_{RPL15A}-*loxP-ble-loxP*-T_{ERG9}	98310	This work
pJT1	pRS425: P_{TEF2}-*ERG20*-T_{RPL3}-P_{TEF1}-*AcNES1*-T_{RPL41B}	98299	(Peng et al., 2017b)
pJT2	pRS425: P_{TEF2}>*ScERG20*^{N127W}>T_{RPL3}–P_{TEF1}>*AcNES1*>T_{RPL41B}	98306	This work
pJT9R	pRS425: T_{RPL3}<*ScERG20*<P_{GAL1}-P_{GAL2}>*AcNES1*>T_{RPL41B}	98305	(Peng et al., 2017a)
pJT10R	pRS425: T_{RPL3}<*ScERG20*^{N127W}<P_{GAL1}-P_{GAL2}>*AcNES1*>T_{RPL41B}	98307	This work
pJT11	pRS425: T_{RPL3}<*ScERG20*^{N127W}<P_{GAL1}-P_{GAL2}>*ClLIS1*>T_{RPL41B}	98308	This work

Table 1. Plasmids used in this work

Symbol > or < indicates the direction of open reading frame.

Table 2. S. cerevisiae *strains used in this work*

Strain	Genotype	Resource/ reference
Saccharomyces cerevisiae		
CEN.PK2-1C	*MATa ura3-52 trp1-289 leu2-3,112 his3Δ 1*	(Entian and Kötter, 1998)
CEN.PK113-5D	*MATa ura3-52*	(Entian and Kötter, 1998)
CEN.PK113-7D	*MATa*	(Entian and Kötter, 1998)
ILHA series strains:		
GH4	oJ3 derivative; *ura3(1, 704)::KlURA3*	(Peng et al., 2015)
GE9S	oJ3 derivative; *ura3(1, 704)::KlURA3-*P_{TEF1}*-yEGFP*	(Peng et al., 2015)
GF6	oJ3 derivative; *ura3(1, 704)::KlURA3-*P_{TEF1}*-UBI4-Degron(F:K3K15)-yEGFP*	This work
GF7	oJ3 derivative; *ura3(1, 704)::KlURA3-*P_{TEF1}*-UBI4-Degron(F:K119S)-yEGFP*	This work
GF8	oJ3 derivative; *ura3(1, 704)::KlURA3-*P_{TEF1}*-UBI4-Degron(F:K113S)-yEGFP*	This work
oURA3	CEN.PK2-1C derivative; *URA3*	(Peng et al., 2017b)
o69	CEN.PK2-1C derivative; *ERG20(-304, 3)::loxP-KlURA3-loxP-*$P_{ERG8[SRE]}$*-UBI4-Degron(F:K3K15)*	This work
oI4	CEN.PK2-1C derivative; *ERG20(-304, 3)::loxP-KlURA3-loxP-*P_{ERG1}*-UBI4-Degron(F:K3K15)*	This work
oP6	CEN.PK2-1C derivative; *ERG20(-304, 3)::loxP-KlURA3-loxP-*P_{ERG2}*-UBI4-Degron(F:K3K15)*	This work
oP8	CEN.PK2-1C derivative; *ERG20(-304, 3)::loxP-KlURA3-loxP-*P_{ERG2}*-UBI4-Degron(F:KN113)*	This work
Oref	oURA3 derivative; [pRS423] [pRS424] [pRS425]	(Peng et al., 2017b)
N6	oURA3 derivative; [pPMVAu8] [pPMVAd3] [pJT1]	(Peng et al., 2017b)
L6	oURA3 derivative; [pPMVAu8] [pPMVAd3] [pJT2]	This work
L669	o69 derivative; [pPMVAu8] [pPMVAd3] [pJT2]	This work
L6I4	oI4 derivative; [pPMVAu8] [pPMVAd3] [pJT2]	This work
L6P6	oP6 derivative; [pPMVAu8] [pPMVAd3] [pJT2]	This work
L6P8	oP8 derivative; [pPMVAu8] [pPMVAd3] [pJT2]	This work
o391	CEN.PK2-1C derivative; *HMG2*^{K6R}*(-152,-1)::HIS3-*T_{EFM1}*<EfmvaS<*P_{GAL1}*-*P_{GAL10}*>ACS2>*T_{ACS2}*-*P_{GAL2}*> EfmvaE >*T_{EBS1}*-*P_{GAL7}	(Peng et al., 2017a)

	pdc5(-31,94)::P_{GAL2}> ERG12>$T_{NAT}P_{TEF2}$>ERG8>T_{IDP1}-T_{PRM9}<MVD1<P_{ADH2}-T_{RPL15A}<IDI1<P_{TEF1}-TRP1	
o401R	o391 derivative; *ERG9(1333, 1335)::T_{URA3}- P_{GAL7}>MVD1>T_{PRM9}-P_{GAL2}>-ERG12>$T_{NAT}T_{IDP1}$<ERG8<P_{GAL10}-P_{GAL1}-IDI1-T_{RPL15A}-loxP-ble-loxP*	This work
o401R0L	o401R derivative; *ERG20(-304, 3)::loxP-KlURA3-loxP-P_{ERG1}*	This work
o401RI4	o410R derivative; *ERG20(-304, 3)::loxP-KlURA3-loxP-P_{ERG1}-UBI4-Degron(F:K3K15)*	This work
N401RA	o401R derivative; *URA3* [pJT9R] *gal80::loxP-kanMX4-loxP*	This work
L401RA	o401R derivative; *URA3* [pJT10R] *gal80::loxP-kanMX4-loxP*	This work
L401RoLA	o401R0L derivative; [pJT10R] *gal80::loxP-kanMX4-loxP*	This work
L401RI4A	o401RI4 derivative; [pJT10R] *gal80::loxP-kanMX4-loxP*	This work
LIM1A	o401R derivative; *URA3* [pJT11] *gal80::loxP-kanMX4-loxP*	This work
LIMI4A	o401RI4 derivative; [pJT11] *gal80::loxP-kanMX4-loxP*	This work

Symbol > or < indicates the direction of open reading frames.

Terpene-producing strains were constructed from *S. cerevisiae* CEN.PK2-1C by transforming plasmid DNA or PCR fragments using the LiAc/PEG/ssDNA method (Gietz and Schiestl, 2007). The *URA3* genotype was generated by transforming the *URA3* fragment amplified from CEN.PK112-7D genomic DNA. *ERG20* was modified on the genome by transforming the PCR fragment R_{ERG20}-*LoxP-KlURA3-LoxP-*$P_{ERG8[SRE]}$-*Degron-*R_{ERG20} (**Appendix 1: Table S1: #26, 27, &28**) or R_{ERG20}-*LoxP-KlURA3-LoxP-*P_{ERG1}-R_{ERG20} (**Appendix 1: Table S1: #30**). Strain o401R was generated from strain o391 by transforming SwaI-digested pIMVAd40R. The gene *gal80* was disrupted by transforming the *loxP-KanMX4-loxP* fragment (**Appendix 1: Table S1: #31**) amplified from plasmid pUG6, and the yeast strains were selected on synthetic complete-glutamate-high-glucose (SCGHG) agar plates with 300 μg mL^{-1} G-418; the nutrient recipe of the SCGHG agar is as follows: 1.6 g L^{-1} uracil-drop-out amino acid mixture (Hanscho et al., 2012), 1.7 g L-1 yeast nitrogen base without ammonium sulfate, 1 g L^{-1} glutamate, 200 g L^{-1} glucose. For terpene-producing strains, at least 3 single clones were stored separately in 20% glycerol at -80 °C as replicates.

2.2 GFP fluorescence and degradation assay

GFP fluorescence was monitored during the early exponential phase (OD_{600} = 0.4 to 0.8) as described previously (Peng et al., 2017b; Peng et al., 2015). Briefly, cells were cultivated aerobically in 20 ml SM-glucose medium in a 100 ml flask and GFP fluorescence was analysed using a BD AccuriTM C6 flow cytometer (BD Biosciences, USA). GFP fluorescence level was expressed as the percentage relative to the background auto-fluorescence from a GFP-negative reference strain GH4 (empty vector integration strain). For the GFP degradation assay, cycloheximide was added into the culture to a final concentration of 50 mg L^{-1}.

2.3 Two-phase flask cultivation

Two-phase flask cultivation was performed as described previously (Peng et al., 2017a; Peng et al., 2017b; Vickers et al., 2015b). Synthetic minimal (SM) medium (containing 6.7 g L^{-1}

yeast nitrogen base, YNB, Sigma-Aldrich #Y0626; pH 6.0) with 20 g L^{-1} glucose as the carbon source was used (SM-glucose). 100 mM 2-(N-morpholino) ethanesulfonic acid (MES, Sigma-Aldrich#M8250) was used to buffer medium pH. Strains were recovered from glycerol stocks by streaking on SM-glucose agar plates (or SGCHG plates for strains with heterologous genes controlled by *GAL* promoters) and pre-cultured in MES-buffered SM medium with 20 g L^{-1} glucose or 40 g L^{-1} glucose (for strains with heterologous genes controlled by *GAL* promoters) as carbon source to exponential phase (cell density OD_{600} between 1 and 4). Two-phase flask cultivation was initiated by inoculating pre-cultured cells to OD_{600} = 0.2 in 25 ml MES-buffered SM-glucose medium; 2 ml dodecane was added to extract terpene products. Flask cultivation was performed at 30 °C and 200 rpm. For all cultivations, about 3 ml culture was sampled before the end of exponential growth phase for OD measurement. For RNA extraction, 2 ml exponential-phase culture (OD_{600} = 1 to 1.5) or 1 ml post-exponential-phase culture (OD_{600} = 10 to 12) was sampled and cells were collected and stored at -80 °C. For analysis of squalene and ergosterol, the cells from the final cultures were washed twice with distilled water and aliquots were stored at -20 °C.

The linear regression coefficients of the *ln* OD_{600} versus time during the exponential growth phase were the maximum growth rates (μ_{max}) (Sonderegger et al., 2004).

2.4 Extraction of ergosterol and squalene

Ergosterol and squalene were extracted using a methanolic pyrogallol saponification as described previously (Peng et al., 2017b). Cell pellets were resuspended in an alkaline methanol solution with internal standard solution and pyrogallol. Saponification was performed at 80 °C. Lipids were extracted with hexane, desiccated, and resuspended in methanol:ethanol (1:1) pyrogallol solution for HPLC analysis.

2.5 Metabolite analysis

Ergosterol, squalene and pyrene were analysed through reverse-phase chromatography as described previously (Peng et al., 2017b). Analytes were eluted isocratically at 1 mL min^{-1} with methanol at 35 °C. Analytes were monitored using a diode array detector (Agilent Technologies) at the following UV wavelengths: 200 nm (for squalene), 274 nm (for ergosterol) and 334 nm (for pyrene).

For linalool and trans-nerolidol analysis, dodecane samples were diluted 40-fold using hexane spiked with a β-pinene internal standard. Diluted samples were analysed with gas chromatography-mass spectrometry as described previously (Peng et al., 2017b). Samples (3 μL) were injected in split mode (ratio 1:30) at 250 °C; analytes were separated on a FactorFour VF-5ms GC column (30m*0.25μm*0.25μm)+10m EZ-guard (Agilent Technologies, PN: CP9013) with 1 mL min^{-1} helium flow and the following oven temperature gradient program: 50 °C for 2 min, +15 °C min^{-1} to 200 °C, 200 °C for 3 min, +40 °C min^{-1} to 325 °C, 325 °C for 0 min. Analytes were ionized and fragmented using electron impact (EI) ionization source and detected by mass spectrometry using a mass selective detector.

An HPLC method, modified from a previous study (Peng et al., 2017a), was used to analyse geraniol, linalool, trans,trans-farnesol, trans-nerolidol, geranylgeraniol, and geranyllinalool.

Dodecane samples from fermentations were diluted in a 40-fold volume of ethanol. These samples (20µl) were analysed using an Agilent 1200 HPLC system with a Zorbax Extend C18 column (4.6 x 150 mm, 3.5 µm, Agilent PN: 763953-902) and a guard column (SecurityGuard Gemini C18, Phenomenex PN: AJO-7597). Analytes were eluted at 35 ^{o}C at 0.9 ml min^{-1} using a mixture of solvent A (high purity water, 18.2 kΩ) and solvent B (45% acetonitrile, 45% methanol and 10% water), with a linear gradient of 90% solvent B from 0-21 min, then 90-100% solvent B from 21-31 min, then 100% from 31-38 min, and finally 5% from 38.1-43 min. Analytes of interest were monitored using a diode array detector (Agilent DAD SL, G1315C) at 202 nm wavelength. Spectral scans were also performed on each of the compounds from 190-400 nm in steps of 2 nm to confirm their identity and purity.

Analytical standards of geraniol (98% purity; Sigma-Aldrich #163333), linalool (97% purity; Sigma-Aldrich #L2602), trans,trans-farnesol (96% purity; Sigma-Aldrich #277541), trans-nerolidol (93.7% purity; Sigma-Aldrich #04610590), limonene (Sigma-Aldrich #W263303), geranylgeraniol (85% purity; Sigma-Aldrich #G3278), and geranyllinalool (95% purity; Sigma-Aldrich #48809), were used to prepare the standard curve for quantification.

2.6 Quantitation of mRNA level

Total RNA was extracted using a TRIzol® Plus RNA Purification Kit (Ambion #12183555). After DNase treatment, 0.2 µg total RNA was used for first-strand cDNA synthesis in a 10 µl reaction using ProtoScript® II Reverse Transcriptase (NEB #M0368). The diluted cDNA was used as the template for quantitative real-time (qRT) PCR (primers are listed in **Appendix 1: Table S1 #33-to-#36**). KAPA SYBR® FAST qPCR Kit (Kapa Biosystems #KP-KK4601) and CFX96 Touch™ Real-Time PCR Detection System (BIO-RAD) were used in qRT-PCR. C_t values were analyzed using CFX Manager Software (Bio-Rad Laboratories, QLD Australia). The actin-encoding gene *ACT1* was used as reference for normalization. Real-time PCR data was analyzed according to the $2^{-\Delta\Delta Ct}$ method (Livak and Schmittgen, 2001).

3. Results

The native FPP synthase (Erg20p) competes with heterologous monoterpene synthases for GPP (**Figure 2a**). Transcriptional down-regulation of Erg20p is ineffective to control carbon competition at this node. Here, we aimed to reduce Erg20p to a minimal level required to maintain sterol flux for normal cell growth, and to re-direct carbon into monoterpene production. The strategy was inspired by the multilevel control seen in ergosterol biosynthesis. *ERG1* is regulated transcriptionally by the sterol-responsive Upc2p transcription factor, which binds at sterol regulatory elements (SREs); in addition, Erg1p is regulated by endoplasmic reticulum-associated protein degradation. Erg20p is a cytosolic protein, with a half-life of >10 hour (Christiano et al., 2014). Destabilization of a cytosolic protein can be engineered by attaching an N-terminal degron, a C-terminal degron, or a PEST sequence (protein destabilizing sequence, rich in Pro, Glu, Ser and Thr) (Jungbluth et al., 2010; Mateus and Avery, 2000; Taxis et al., 2009). Degron-mediated degradation can be tuned due to a range of available sequences with differing efficiency for protein destabilisation; degrons are also short sequences that are easily introduced at protein termini.

3.1 Testing the N-end rule by destabilising GFP using N-degrons

To engineer a destabilized Erg20p, we applied the N-degron-mediated protein degradation mechanism, known as the N-end rule pathway (Bachmair et al., 1986; Suzuki and Varshavsky, 1999). A ubiquitin moiety, an N-end rule residue, and a lysine-asparagine spacer (together the 'degron') were sequentially fused to the N-terminus of a protein (**Figure 2a**), following a previously-developed model (Suzuki and Varshavsky, 1999). The resulting fusion protein is hydrolysed by ubiquitin C-terminal hydrolase and the N-end rule residue is exposed, leading to ubiquitination on the lysine-asparagine spacer and the further protein degradation through the proteasome (**Figure 2a**).

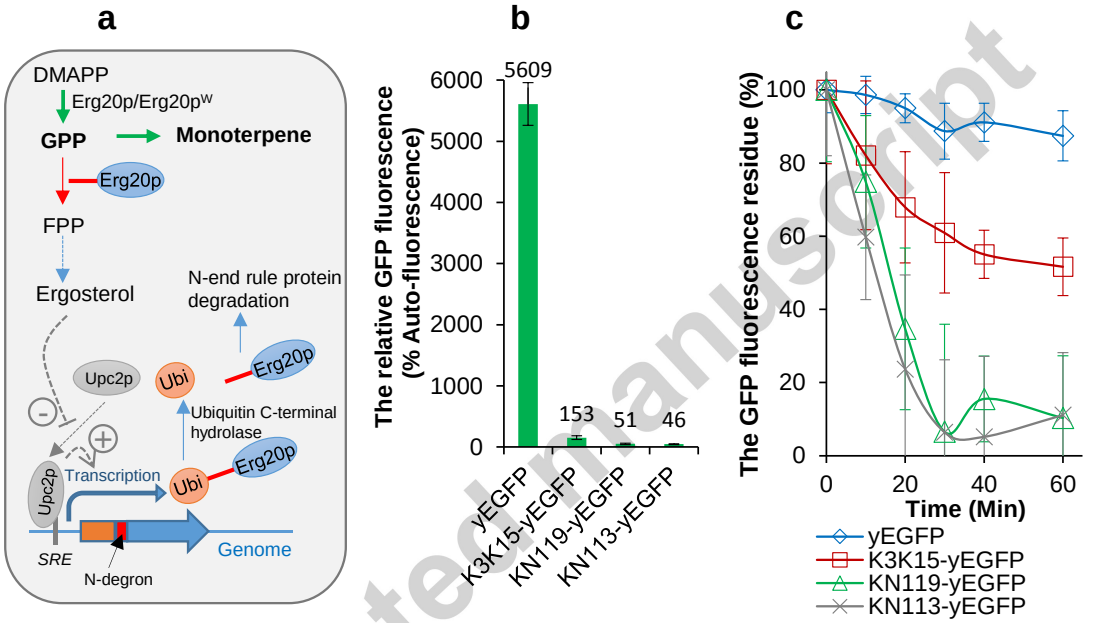

Figure 2. Schematic representation of engineered regulation on farnesyl pyrophsophate synthase Erg20p (a) and N-degron-dependent degradation of green fluorescent protein GFP (b & c) in yeast. (a) The mechanism for *ERG20* regulation, including N-degron-dependent protein degradation and Upc2p-dependent sterol responsive transcriptional regulation: DMAPP, dimethylallyl pyrophosphate; IPP, isopentenyl pyrophosphate; GPP, geranyl pyrophosphate; FPP, farnesol pyrophosphate; Erg20p, FPP synthase; Erg20pW, FPP synthase mutant N127W; UBI/Ubi, ubiquitin. (b) GFP fluorescence levels in the strains (GE9S, GF6, GF7, and GF8) expressing the reference yEGFP, or the yEGFP fused with N-degron K3K15, KN119 or KN113. (c) GFP degradation analysis after adding cycloheximide. Mean values ± standard deviations are shown (N = 3).

Protein degradation using three different degrons was tested using yeast enhanced green fluorescent protein (yEGFP) as the reporter protein (**Figure 2b & 2c**). GFP fluorescence is easily detected using a flow cytometer for high throughput and can provide a rapid response read-out (Peng et al., 2015) and is usually a very stable protein (**Figure 2c**), making it ideal for the current application. The three degrons tested (K3K15, KN119 and KN113) have a Phe residue as the N-end rule residue and additional 14-residue lysine-asparagine spacer which attracts different levels of ubiquitination and thus result in differing protein degradation rates

(Suzuki and Varshavsky, 1999). N-degron-yEGFP tagging resulted in dramatically decreased GFP fluorescence compared to the un-tagged yEGFP control (**Figure 2b**). Consistent with a previous study using β-glucosidase as a reporter protein (Suzuki and Varshavsky, 1999), the K3K15 degron was the least effective at decreasing fluorescence. No significant difference was observed in fluorescence levels between the KN119 and KN113 degron constructs (two-tailed t-test $p > 0.5$). GFP protein turnover was tested by monitoring the fluorescence change after cycloheximide was added to stop protein translation (**Figure 2c**). The yEGFP:K3K15 construct exhibited a protein half-life of 1 hour, and the yEGFP:KN119 and yEGFP:KN113 constructs exhibited protein half-lives of ~ 15 min. Due to These data confirm that N-degron fusions can be used to destabilize a cytosolic protein and parameterised the degrons tested under our conditions.

3.2 Engineering flux balance demand control at *ERG20* for improved monoterpene production

The dramatic destabilisation observed in degron-tagged GFP is unlikely to be useful as a flux modulation approach at the FPP synthase node because the resulting protein levels are likely to be too low to sustain sufficient flux to sterols, which are required for cell wall production and normal growth. However, as noted, previous attempts to engineer transcriptional down-regulation of Erg20p for increased monoterpene production by replacing the native promoter with down-regulatable promoters were unsuccessful (Zhao et al., 2016; Zhao et al., 2017). To balance the severe effect of the degron-mediated degradation, we applied a feedback-regulation mechanism by exploiting sterol responsive transcription elements to increase transcription under decreased ergosterol conditions. This was combined with the protein degradation approach with the aim of achieving a balance between maintenance of cell growth and minimising Erg20p activity, and thereby obtaining flux-demand control over this node (**Figure 2a**).

The *ERG20* promoter does not respond to ergosterol concentration, whereas *ERG2*, *ERG1*, and *ERG8* do (Dimster-Denk et al., 1999; Kuranda et al., 2010; Vik and Rine, 2001). Transcript analysis under normal conditions demonstrates a relative transcript abundance of:

$$ERG2 >> ERG20 \approx ERG1 >> ERG8 \text{ (Christiano et al., 2014);}$$

in low ergosterol conditions, transcription from ergosterol-responsive promoters is up-regulated ~ 10-fold (Dimster-Denk and Rine, 1996; Vik and Rine, 2001). The genomic *ERG20* gene was modified by fusing an N-degron to the Erg20p N-terminus and replacing the promoter with a sterol responsive promoter. We tested the *ERG8* promoter (P_{ERG8}), the *ERG8* promoter with additional SRE sequence inserted ($P_{ERG8[SRE]}$), the *ERG1* promoter (P_{ERG1}), and the *ERG2* promoter (P_{ERG2}); in combination with degrons K3K15, KN119, and KN113 (see above; **Figure 2**), making a total of 12 target promoter:degron combinations. Yeast transformants were successfully isolated for five combinations: $P_{ERG8[SRE]}$-K3K15, P_{ERG1}-K3K15, P_{ERG2}-K3K15, P_{ERG2}-KN119, and P_{ERG2}-KN113. We presume that the other combinations were lethal, perhaps due to insufficient sterol production. In support of this, we observed that the weakest degron (K3K15) combined with all of the promoters except for the weakest promoter (P_{ERG8}) successfully yielded transformants; and that the strongest promoter (P_{ERG2}) worked with all of the degrons. Addition of an extra SRE was required to successfully

retrieve transformants for the *ERG8* promoter ($P_{ERG8[SRE]}$). For those combinations that were successful, we noted that positive transformants formed smaller colonies on the selective plates than false-positive transformants (data not shown).

In order to investigate the effect of these modifications on monoterpene production, three plasmids were introduced into the *ERG20* control strain (CEN.PK2-1 derivative oURA3; Table 2) and the *ERG20*-modified strains (promoter replacement and degron tagged) described above (Table 2). Mevalonate pathway flux to the C5 isoprenoid precursors IPP and DMAPP was increased by introducing two plasmids expressing upper and lower MVA pathway modules (pPMVAu8 and pPMVAd3, respectively; Table 1 and Figure 1) which we have previously used to improve sesquiterpene titres (Peng et al., 2017b). The terpene synthetic pathway plasmid pJT2 was used as a flux reporter. pJT2 contains two genes: (a) a mutant Erg20p^{N127W} (Erg20p^{W}, encoded by *ERG20*^{W}) engineered to exclude FPP from its active site and thus release the GPP moiety, which accumulates GPP as the product (Ignea et al., 2013), and (b) a *trans*-nerolidol synthase (*AcNES1*) from *Actinidia chinensis*, which has both sesquiterpene synthase activity (producing nerolidol from FPP) and monoterpene synthase activity (producing linalool from GPP) (Green et al., 2012). *AcNES1* can therefore act as a reporter for both GPP and FPP availability. These modifications resulted in strains with either non-modified or promoter/degron-modified *ERG20*, as well as an up-regulated mevalonate pathway and a monoterpene/sesquiterpene reporter system (Table 2).

Previously, we used a similar set of plasmids with a native *ERG20* (P_{ERG20}-*ERG20*) instead of the mutant Erg20p^{W} in the reporter plasmid to engineer increased FPP for sesquiterpene production. The resulting strain N6 produced 56 mg L^{-1} of the sesquiterpene nerolidol and farnesol production was below the detection limit (Peng et al., 2017b). We examined strain N6 for linalool production and it was not detected (**Figure 3a**), confirming that in this strain, GPP is not generally available for conversion into monoterpenes. Replacing *ERG20* with *ERG20*^{W} in the terpene synthetic module resulted in a slight but not significant decrease in nerolidol (two tailed t-test $p > 0.1$), and production of 0.4 mg L^{-1} monoterpene linalool in the new strain L6 (**Figure 3a**). Strain N6 grows at about half the rate of the control strain without engineering (μ_{max} of ~0.15 compared to 0.3 h^{-1}; (Peng et al., 2017b)). Interestingly, strain L6 showed faster growth (μ_{max} of ~0.2 h^{-1}) than strain N6 (**Figure 3b & 3d**).

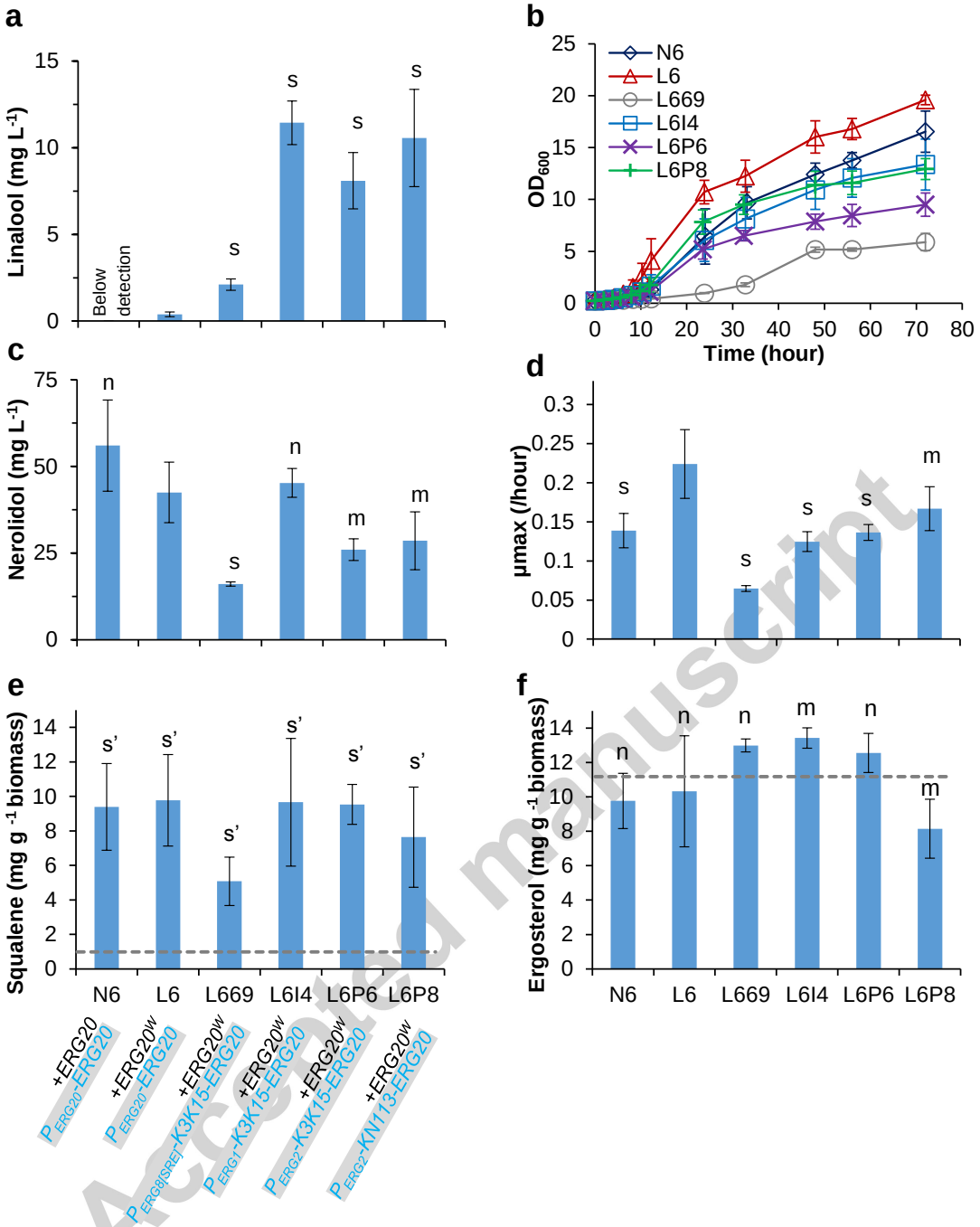

Figure 3. Characterisation of the strains overexpressing the mevalonate pathway and nerolidol/linalool synthetic module [*ERG20*$^{(W)}$+*AcNES1*] using constitutive promoters and with/without the genomic *ERG20* modified. (a) Linalool titres at 72 hour. (b) Growth curves over the batch cultivation. (c) nerolidol titres at 72 hour. (d) Maximum specific growth rates (μ_{max}) during the exponential phase. (e) Intracellular squalene contents. (f) Intracellular ergosterol contents. Dash lines in e & f show the squalene and ergosterol levels in the reference strain Oref without mevalonate pathway enhanced. Mean values ± standard deviations are shown (N = 3). Data for strains N6 and Oref was published in our previous study (Peng et al., 2017b). Linalool and nerolidol were analyzed using GC-MS. For a, c &d, two-tailed Welch's t-test was used for statistical analysis relative to L6: n, $p > 0.1$; m, $p \in [0.05, 0.1]$; s, $p < 0.05$. For e & f, two-tailed Welch's t-test was used for statistical analysis of log-transformed data (n' and s') or original data (n, m, and s) relative to Oref: n'/n, $p > 0.1$; m', $p \in [0.05, 0.1]$; s'/s, $p < 0.05$.

The same three plasmids (upper and lower MVA modules; and ERG20^{W}+*AcNES1*) were introduced into the strains with the genomic *ERG20*-modifications to generate strain L669 ($P_{ERG8[SRE]}$-*K3K15-ERG20*), L6I4 (P_{ERG1}-*K3K15-ERG20*), L6P6 (P_{ERG2}-*K3K15-ERG20*), and L6P8 (P_{ERG2}-*KN113-ERG20*) (**Figure 3**). All of these strains exhibited increased linalool production compared to strain L6 (two-tailed t-test $p < 0.05$; **Figure 3a**). The highest average linalool titres achieved were ~11 mg L^{-1} in the P_{ERG1}-*K3K15-ERG20* and P_{ERG2}-*KN113-ERG20* strains. Growth and nerolidol titres in these strains were variable (**Figure 3b, 3c & 3d**). The $P_{ERG8[SRE]}$-*K3K15-ERG20* strain showed dramatically impaired growth and reduced nerolidol titre, as well as having the lowest linalool titre of the chromosomally engineered strains. The other strains (P_{ERG1}-*K3K15-ERG20*, P_{ERG2}-*K3K15-ERG20* and P_{ERG2}-*KN113-ERG20*) still produced > 25 mg L^{-1} nerolidol; maximum growth rates in these strains were similar to strain N6, but lower than strain L6 (Figure 3). These data demonstrate that the *ERG20* modifications examined increased monoterpene production but did not eliminate sesquiterpene production. Moreover, growth rates were still negatively impacted. They also demonstrate that different promoter/degron combinations resulted in different carbon balance between the C10 and C15 products.

3.3 Squalene and ergosterol content in *ERG20*-modified strains

In our previous study, overexpressing the MVA modules resulted in squalene accumulation in the sesquiterpene strain N6 compared to the wild-type strain Oref (dashed line in Figure 4e), indicating excess FPP was converted to squalene instead of sesquiterpene (Peng et al., 2017b). Strain L6 exhibited a similarly increased squalene content (**Figure 3e**), suggesting in the presence of upstream pathway engineering, excess FPP is produced and converted to squalene (as well as sesquiterpene). Likewise, all of the genomic *ERG20*-modified strains (L669, L6I4, L6P6 and L6P8) had increased squalene content relative to the control strain. These data indicate that excess carbon is overflowing into squalene production in all of the strains. However, in the case of strain L669, ($P_{ERG8[SRE]}$-*K3K15-ERG20*; the weakest promoter combined with the weakest degron), squalene accumulation was about half that compared to N6 and L6 (log-transformed data; one-tailed t-test $p < 0.05$). As noted above, the growth rate in this strain was also very low (**Figure 3b & 3d**); there is no apparent reason for this considering that sufficient squalene and ergosterol is available (**Figure 3e & 3f**). Ergosterol content in the *ERG20*-modified strains was not significantly different to the control strain Oref (dashed line in Figure 4f) and strain L6 (**Figure 3f**).

3.4 Engineering *ERG20* for improved monoterpene production in high-level sesquiterpene-producing background strain

The promoters used to drivheterologous genes in the above constructs have decreased expression activities in the post-exponential phase (Peng et al., 2015), resulting in decreased productivities (Peng et al., 2017a). We have previously shown that sesquiterpene productivity can be improved by using diauxie-inducible *GAL* promoters in a *gal80Δ* background strain instead of constitutive promoters (Peng et al., 2017a). When *GAL* promoters were used, the resulting strain N391DA produced 400 mg L^{-1} nerolidol in flask cultivations (Peng et al.,

2017a). In this strain, we observed mevalonate accumulation (unpublished data), suggesting that the lower MVA pathway is a flux bottleneck. This is probably due to the upstream module being controlled by *GAL* promoters while the downstream module was still controlled by constitutive promoters. We therefore first constructed a new background strain from the N391DA parent strain o391 (**Table 1**) by introducing a copy of the lower-part MVA pathway module controlled by *GAL* promoters (the pIMVAd40R plasmid, producing strain o401R; **Table 2**). The *gal80* disruption and a P_{GAL}-controlled *ERG20+AcNES1* module (pJT9R; **Table 1**) were introduced to generate a terpene production strain (strain N401RA; **Table 2**). This strain N401RA has all heterologous genes (upper and lower MVA pathway and *ERG20+AcNES1* terpene production module) controlled by *GAL* promoters. Similar to strain N391DA from our previous study, strain N401RA produced ~ 400 mg L^{-1} nerolidol at 72 h (**Figure 4d**). It also produced ~20 mg L^{-1} of the C15 isoprenoid alcohol farnesol and ~15 mg L^{-1} of the C20 isoprenoid alcohol geranylgeraniol (**Figure 4c & 4e**), which are commonly produced by endogenous non-specific hydroxylation in the presence of excess FPP/GGPP (Farhi et al., 2011; Peng et al., 2017b). This suggests that excess prenyl phosphate was dephosphorylated instead of being converted into nerolidol. No monoterpenes (linalool and geraniol) were detected, as expected considering the absence of dedicated GPPS activity in this strain; and growth rate was unaffected (**Figure 4f**).

Swapping the *ERG20* gene with the GPP-producing $ERG20^{W}$ mutant (pJT10R, to make strain L401RA**; Table 2**) resulted in production of small amounts of the monoterpenes linalool (~1.0 mg L^{-1}) and geraniol (the hydrolysis product of GPP; ~0.15 mg L^{-1}) (**Figure 4a & 4b**). Neither growth nor production of sesquiterpene and diterpene products (farnesol, nerolidol, and geranylgeraniol) were significantly different in this strain (**Figure 4c-4f**).

The genomic *ERG20* gene was further engineered by replacing the promoter with the sterol-regulative promoter, P_{ERG1} (similar transcriptional strength to the *ERG20* promoter; no degron; strain L401RoLA) or with P_{ERG1}:K3K15 degron (weakest degron; strain L401RI4A). Strain L401RoLA exhibited very slight increase in monoterpene production (linaool, ~1.7 mg L^{-1} and geraniol, ~0.22 mg L^{-1}) compared to strain L401RA (**Figure 4a & 4b**), but no significant change in sesquiterpene and diterpene production (**Figure 4c-4e**). A decreased maximum growth rate (0.18 h^{-1}) relative to N401RA and L401RA was also observed (**Figure 4f**).

A remarkable increase in monoterpene production (~18 mg L^{-1} linalool and ~16 mg L^{-1} geraniol, >18-fold more than the reference L401RA) was observed in strain L401RI4A (**Figure 4a & 4b**), accompanied by a significant decrease in sesquiterpene (nerolidol and farnesol) and diterpene (geranylgeraniol) production (**Figure 4c-4e**). This strain also exhibited a sharp decrease in growth rate, to ~0.09 h^{-1} (**Figure 4f & 4g**).

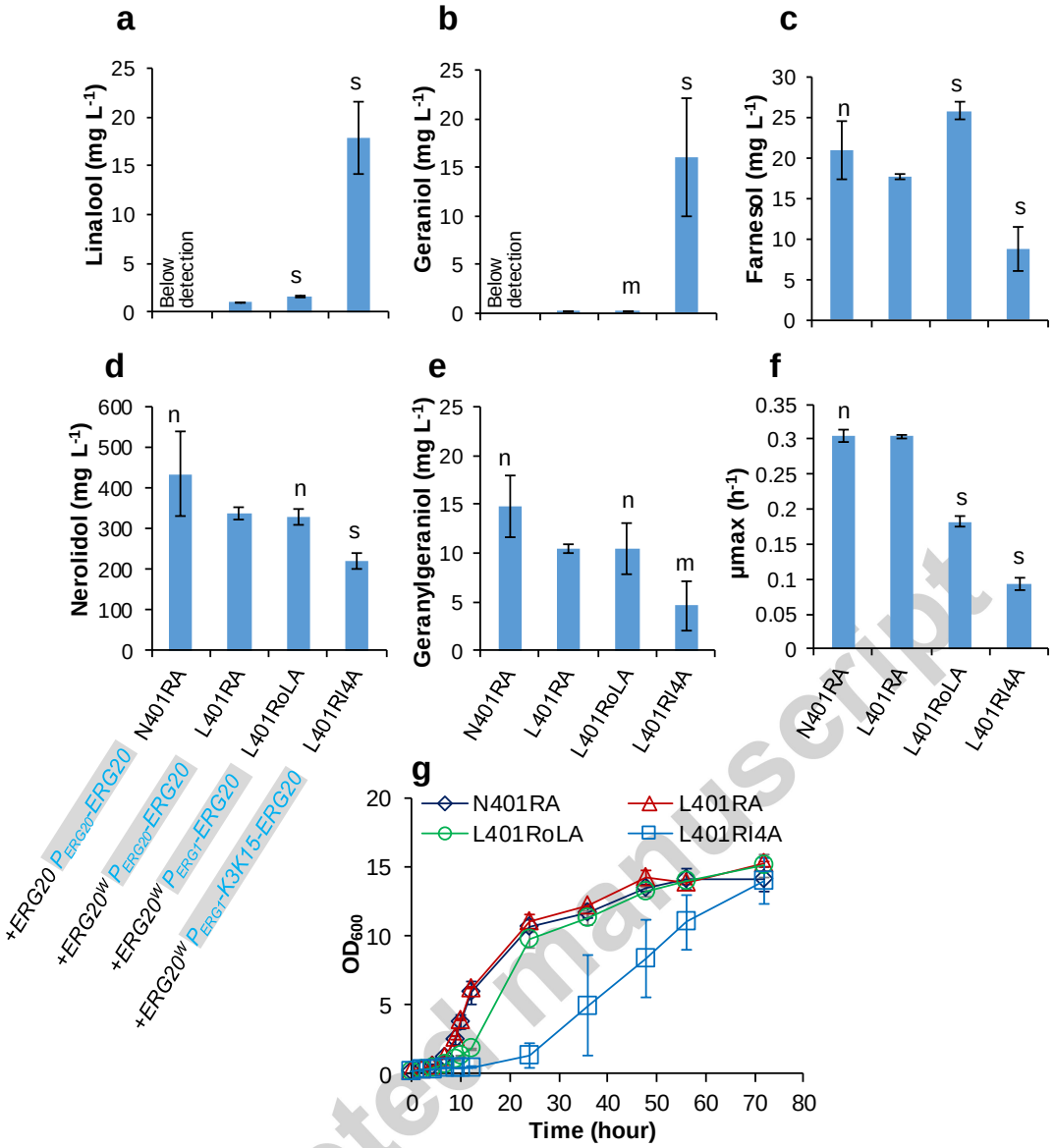

Figure 4. Characterisation of the strains overexpressing the mevalonate pathway and nerolidol/linalool synthetic genes [*ERG20*$^{(W)}$+*AcNES1*] using diauxie-inducible promoters and with/without modifying the genomic *ERG20*. (a) Linalool titres, (b) geraniol titres, (c) farnesol titres, (d) nerolidol titres, and (e) geranylgeraniol titres at 72 hour. (f) Maximum specific growth rates (μ_{max}) during the exponential phase. (g) Growth curves over batch cultivation. Terpenes were analyzed using the LC-UV method. Mean values ± standard deviations are shown (N = 3). Two-tailed Welch's t-test was used for statistical analysis relative to L401RA: n, $p > 0.1$; m, $p \in [0.05, 0.1]$; s, $p < 0.05$.

3.5 Transcriptional response of sterol-responsive genes in genomic *ERG20*-modified strains

To examine transcriptional responses to *ERG20* promoter modification, we performed quantitative real-time PCR using strains N401RA (overexpressed *ERG20*, no genomic *ERG20* modification), L401RA (*ERG20*^{W}, no genomic *ERG20* modification), L401RoLA (*ERG20*^{W}, P_{ERG20} replaced with P_{ERG1}), and L401RI4A (*ERG20*^{W}, P_{ERG20} replaced with $P_{ERG1;}$ K3K15

degron). Expression of the genomic ERG20 and the overexpressed *ERG20* or *ERG20*^{W} cannot be differentiated using this approach, so there should be no difference between strains N401RA and L401RA (control experiment). However, if a sterol response is present, it should be observable in the other sterol-responsive genes, including squalene epoxidase (*ERG1*) and C-8 sterol isomerase (*ERG2*). mRNA levels for these genes were examined (**Figure 5**). *ACT1* was used as the reference gene for normalization. *PDA1* was used as a second reference gene for method validation. Strain data was normalized to N401RA (i.e. the other strain data is presented as fold-change relative to N401RA). In both exponential and ethanol growth phases, *PDA1* transcript level was not significantly different between N401RA and the other three strains, confirming that the *ACT1* normalization was appropriate across cultivation phases. *ERG1* and *ERG2* mRNA levels were also similar between N401RA and L401RA in both fermentation stages. In the exponential phase, *ERG1* and *ERG2* transcript levels were lower (significant only for *ERG2*) in genomic *ERG20*-modified strains L401RoLA and L401RI4A relative to the *ERG20* unmodified strains; whereas in the ethanol growth phase, *ERG1* and *ERG2* transcription was higher. This suggests that, if a response was present, it occurred in the ethanol phase but not in the exponential phase.

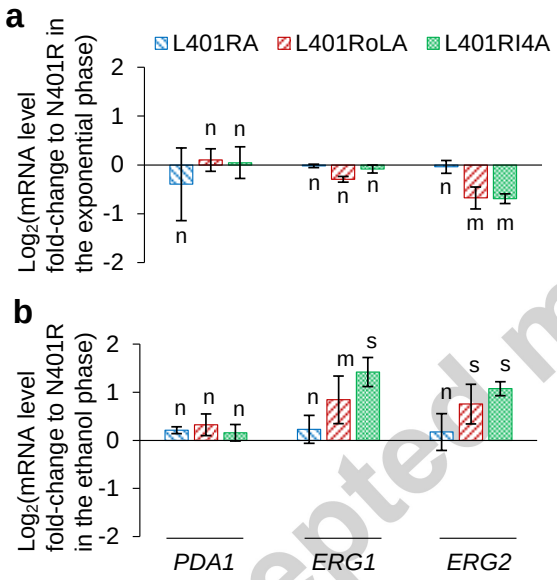

Figure 5. Analysis of mRNA levels in the exponential growth phase (a) and the ethanol growth phase (b). Data were normalized using the reference *ACT1* data in the exponential or ethanol growth phase, separately. Mean values ± standard deviations are shown (N = 3). Two-tailed Welch's t-test was used for statistical analysis relative to N401R: n, $p > 0.1$; m, $p \in [0.05, 0.1]$; s, $p < 0.05$.

3.6 Producing limonene in *ERG20*-engineered strain

Limonene is an interesting monoterpene product that can be used as fragrance, organic solvent, chemical precursor, and a component of renewable aviation fuels (Brennan et al., 2012). Here, limonene production was evaluated using two of the intensively engineered background strains described above. The limonene synthesis plasmid included *ERG20*^{W} and *Citrus limon* limonene synthase (*ClLS*; (Behrendorff et al., 2013)), both under the control of

GAL promoters (pJT11; **Table 2**). Strains LIM1A (native genomic *ERG20*) and LIMI4A (P_{ERG1}-*K3K15:ERG20*) were generated by transforming this plasmid into strains o401R and o401RI4 (**Table 1**), which have a *GAL* promoter-controlled overexpressed MVA pathway.

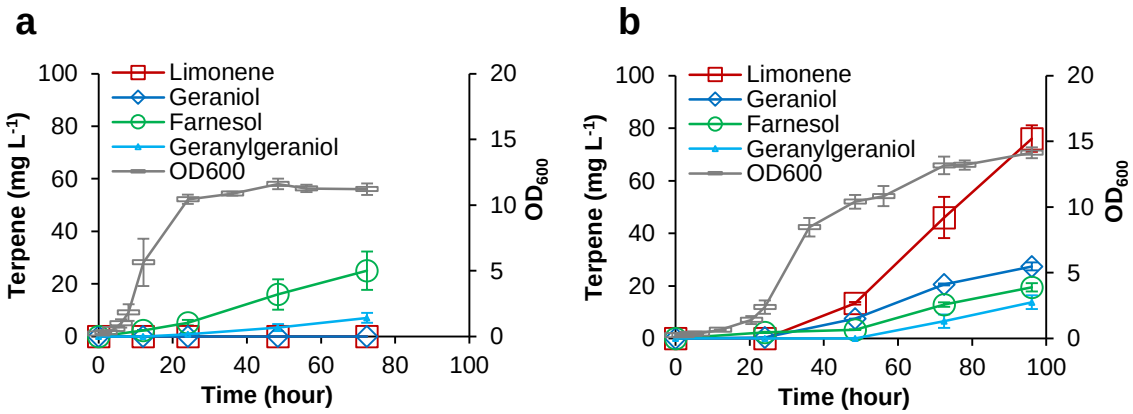

Figure 6. Characterisation of the strains overexpressing mevalonate pathway and limonene synthetic gene (*ERG20*^{W}+*ClLIS1*) using diauxie-inducible promoters. (a) Strain LIM1A (without engineering on genomic *ERG20*). (b) Strain LIMI4A (with genomic *ERG20* modified into P_{ERG1}-*K3K15-ERG20*). Mean values ± standard deviations are shown (N = 2).

Similar to the nerolidol/linalool-producing strains (L401RA and L401RI4A; **Figure 4**), the genomic modification of *ERG20* lead to decreased exponential growth rate in strain LIMI4A (μmax = 0.10 h^{-1}), compared to strain LIM1A (μmax = 0.28 h^{-1}; **Figure 6**). Strain LIM1A exhibited a different growth defect: cell division stopped after 24 hour (**Figure 6a**), whereas strain LIMI4A continued to grow in the post-exponential phase (**Figure 6b**). Although growth stopped in LIM1A, farnesol and geranylgeraniol accumulation increased in the post-exponential phase (**Figure 6a**), showing that the post-exponential cells are still metabolically active despite not undergoing cell division. Monoterpene production (limonene and geraniol) was below detection in LIM1A (**Figure 6a**). In contrast, monoterpenes limonene and geraniol, as well as farnesol and geranylgeraniol, were produced in genomic *ERG20*-engineered strain LIMI4A (**Figure 6b**). Geraniol titre was 27 mg L^{-1} at 96 hour, and limonene titre was ~76 mg L^{-1}.

4. Discussion

While sesquiterpenes have been successfully produced at high g/L titres (Meadows et al., 2016; Peng et al., 2017a), monoterpene production lags far behind. The best monoterpene titres have been achieved in *E. coli* (e.g. limonene was produced up to 400 mg L^{-1} from 10 g L^{-1} glucose in *E. coli* (Alonso-Gutierrez et al., 2013)), while production in yeast remains challenging. It is thought that the high level limonene production in *E. coli* might result from effective competition by the limonene synthase with the native *E. coli* FPP synthase (Willrodt et al., 2014), an unusual situation given the relatively poor kinetic properties of most terpene synthases. In yeast, it seems likely that the FPP synthase outcompetes the heterologous monoterpene synthases for GPP. A titre of 85 mg L^{-1} linalool was recorded in *S. cerevisiae* strain with enhanced MVA pathway flux, an *erg9Δ* mutation, chromosomal replacement of

the FPP synthase (Erg20p) with a GPP-accumulating mutant, and overexpressing an additional GPP-accumulating FPP synthase mutant and a strawberry (*Fragaria* × *ananassa*) nerolidol synthase from a plasmid (Zhuang, 2013). However, this strain showed a dramatic growth deficiency and required a 14-day cultivation (20 g L^{-1} glucose) to obtain this titre. In other engineered microbial strains, linalool production titres remain in the μg L^{-1} scale (Amiri et al., 2016; Rico et al., 2010). The highest titres for other monoterpenes in batch cultivation in engineered microorganisms are currently 41 mg L^{-1} for sabinene in *E.coli* (Zhang et al., 2014), 32 mg L^{-1} for pinene in *E.coli* (Sarria et al., 2014), 66 mg L^{-1} for geraniol in *S. cerevisiae* (Zhao et al., 2016), 69 mg L^{-1} for geraniol in *E.coli* (Liu et al., 2016), and 24 mg L^{-1} for limonene in *Yarrowia lipolytica* (Cao et al., 2016).

In this study, we first improved upstream pathway flux to increase the availability of prenyl phosphates, then engineered at the flux-competing enzyme, FPPS. Transcriptional regulation has previously been shown to be inadequate to control flux competition at FPPS (Zhao et al., 2016; Zhao et al., 2017). FPPS is a very stable protein (Christiano et al., 2014), and this may help mitigate down-regulation through transcriptional regulation. We instead applied regulation at the protein level through the N-end-rule protein degradation mechanism. We also implemented an ergosterol-responsive transcriptional up-regulation mechanism designed to engage if the cellular ergosterol levels became too low (which might cause a growth defect). This regulatory engineering increased monoterpene production in strains with either constitutively overexpressed monoterpene synthetic pathways or inductively overexpressed monoterpene synthetic pathways. The highest titres achieved here were 18 mg L^{-1} for linalool and 76 mg L^{-1} limonene. This is the highest currently-reported titre for limonene in yeast.

Although leading to improved monoterpene production, the current strategy did not eliminate the accumulation of sesquiterpenes, diterpenes, and squalene (**Figures 3, 4, & 6**). In our previous study, down-regulating the native squalene synthase by protein destabilization strongly re-directed carbon from the sterol pathway into sesquiterpene production (Peng et al., 2017b). In contrast, down-regulation of the native *ERG20* in the current study did not have a particularly strong effect on downstream metabolites (squalene, ergosterol, and sesquiterpenes), although it did increase monoterpene production, which was the aim. The $ERG20^{W}$ mutant which was introduced to increase GPP availability still has FPP synthase activity (Ignea et al., 2013); this may have provided sufficient flux to maintain downstream intermediate pools despite the decrease in FPPS activity derived from the native chromosomal gene.

The accumulation of terpene alcohols such as geraniol, farnesol, and geranylgeraniol, has been shown in previously studies (Farhi et al., 2011; Peng et al., 2017b; Zhao et al., 2016), and is likely coupled with increased intracellular concentrations of prenyl pyrophosphate precursors. Production of these terpene alcohols can be attributed to dephosphorylation of prenyl pyrophosphate precursors through enzymatic catalysis or non-enzymatic reactions, whereas potential enzymatic mechanisms include hydrolysis by endogeneous phosphatases such as Dpp1p and Lpp1p (Scalcinati et al., 2012; Tokuhiro et al., 2009) and solvolysis by prenyl transferases such as GPP synthase and FPP synthase (Poulter and Rilling, 1976; Saito and Rilling, 1979).

We hypothesised that sterol-responsive transcriptional regulation through the Upc2p transcription factor might be activated in *ERG20*-modified strains to complement protein

degradation, resulting in a balance to maintain ergosterol concentration. To examine this more carefully, we looked at the transcriptional profile of *ERG* genes in engineered strains. Because of the plasmid-mediated expression of *ERG20* or $ERG20^{W}$, we could not specifically measure transcriptional change of the genomic *ERG20*; however, we looked at the sterol-responsive genes *ERG1* and *ERG2* in *ERG20*-modified strains. The transcription levels in both P_{ERG2}-*K3K15-ERG20* and P_{ERG1}-*ERG20* strains (L401RI4A and L401RoLA) decreased (though not significantly) in the exponential phase, and increased by ~1-fold in the post-exponential phase (**Figure 5**). This suggests that the Upc2p-mediated sterol responsive regulation was activated, but only in the post-exponential phase; and not as dramatically as shown in previous studies where the enzymatic inhibitors were added to constrain sterol synthesis (Vik and Rine, 2001).

In previous studies, the growth profiles of engineered monoterpene-producing yeast strains were not compared (Amiri et al., 2016; Liu et al., 2013; Zhang et al., 2014; Zhao et al., 2016). Here, we showed that the growth of engineered strains was strongly influenced by the different genetic engineering approaches. **(1)** Strain L6 ($ERG20^{W}$ mutant overexpressed; μ = 0.22 h^{-1}) exhibited faster exponential growth rate than strain N6 (native *ERG20* is overexpressed μ = 0.14 h^{-1}; **Figure 3**). **(2)** Genetic modifications on genomic *ERG20* decreased the exponential growth rate, including the genotypes $P_{ERG8[SRE]}$-*K3K15-ERG20* (strain L669), P_{ERG1}-*K3K15-ERG20* (strain L6I4 & L401RI4A), P_{ERG2}-*K3K15-ERG20* (strain L6P6), P_{ERG2}-*KN113-ERG20* (strain L6P8), and even the genotype P_{ERG1}-*ERG20* (strain L401RoLA), which had no N-degron-dependent protein destabilization of Erg20p (**Figure 3 & Figure 4**). **(3)** Cell growth for strain LIM1A (limonene production plasmid with native *ERG20* overexpressed) halted in the post-exponential phase (**Figure 6**), suggesting severe metabolic imbalance. These results indicate that flux control at the Erg20p node is a critical determinant of cell growth.

Product toxicity is probably not the cause of the observed growth defects, because linalool titres (**Figure 3**) were below toxic levels (**Appendix 1: Figure S1**) and in any case, addition of a dodecane extraction phase such as we used alleviates monoterpene toxicity (Brennan et al., 2012). Genomic *ERG20*-engineered strains still accumulated FPP-derivative products (squalene, nerolidol, and geranylgeraniol) at much higher levels than the control (**Figure 3 & 4**), which suggests that the decreased growth rate was not caused by insufficient metabolic flux to FPP.

In contrast to the nerolidol/linalool-producing strains having both GPP-and-FPP-sink pathways (via dual-activity nerolidol synthase), the limonene strains LIM1A and LIMI4A only harbor a heterologous GPP-sink pathway (via limonene synthase). Strain LIM1A showed a normal exponential growth, but growth halted in the post-exponential phase (**Figure 6a**). In contrast, strain LIMI4A showed inhibited exponential growth (presumably due to the genomic *ERG20* modification), and a normal post-exponential growth (**Figure 6b**). In these strains, enhancement of MVA pathway flux from overexpressed genes was regulated by diauxie-inducible promoters, which are strongly enhanced in the post-exponential phase but not the exponential phase (Peng et al., 2017a). Considering this, it is possible that growth arrest in LIM1A might be due to accumulation of intracellular FPP in the post-exponential phase. This is supported by production of farnesol in this phase (**Figure 6a**). The engineering on genomic *ERG20* in LIMI4A partially re-directed the flux from FPP synthesis to the GPP sink (limonene) pathway (**Figure 6b**). This might alleviate the toxicity caused by FPP

accumulation. In support of this, strain LIMI4A produced less farnesol compared to strain LIM1A (**Figure 6b vs. 6a**).

5. Conclusion

N-degron-mediated protein degradation and sterol-responsive transcriptional regulation were engineered to regulate genomic FPP synthase Erg20p, with the aim of redirecting carbon flux toward monoterpene synthesis. This regulatory strategy increased monoterpene production in the strains, in which heterologous monoterpene synthetic pathway genes were overexpressed under the control of either constitutive promoters or diauxie-inducible promoters. Titres of 18 mg L^{-1} linalool or 76 mg L^{-1} limonene were reached in engineered strains using 20 g L^{-1} glucose. However, we found that engineered strains still produced considerable amounts of non-targeted products, geraniol, farnesol and geranylgeraniol; and that engineering on the genomic Erg20p engineering inhibited exponential growth. We postulate that an imbalance in synthesis of prenyl pyrophosphate (possibly accumulation of FPP) might cause growth inhibitions. Future work will focus on investigating this hypothesis. In summary, this strategy can be applied with further novel and combinatorial engineering strategies for economic/efficient production of monoterpene in yeast.

Acknowledgements

BP was supported by a University of Queensland International Postgraduate Research Scholarship. CEV was supported by Queensland Government Smart Futures and Accelerate Fellowships. Metabolite analysis was performed in the Metabolomics Australia Queensland Node. We thank Dr Manuel R. Plan for HPLC analysis and Dr Panagiotis Chrysanthopoulos for GC analysis.

References

Alonso-Gutierrez, J., Chan, R., Batth, T. S., Adams, P. D., Keasling, J. D., Petzold, C. J., Lee, T. S., 2013. Metabolic engineering of Escherichia coli for limonene and perillyl alcohol production. Metabolic engineering. 19**,** 33-41.

Amiri, P., Shahpiri, A., Asadollahi, M. A., Momenbeik, F., Partow, S., 2016. Metabolic engineering of Saccharomyces cerevisiae for linalool production. Biotechnology letters. 38**,** 503-8.

Anderson, M. S., Yarger, J. G., Burck, C. L., Poulter, C. D., 1989. Farnesyl diphosphate synthetase. Molecular cloning, sequence, and expression of an essential gene from *Saccharomyces cerevisiae*. The Journal of biological chemistry. 264**,** 19176-84.

Bachmair, A., Finley, D., Varshavsky, A., 1986. *In vivo* half-life of a protein is a function of its amino-terminal residue. Science. 234**,** 179-86.

Behrendorff, J. B. Y. H., Vickers, C. E., Chrysanthopoulos, P., Nielsen, L. K., 2013. 2,2-Diphenyl-1-picrylhydrazyl as a screening tool for recombinant monoterpene biosynthesis. Microb Cell Fact. 12**,** 76.

Brennan, T. C., Turner, C. D., Kromer, J. O., Nielsen, L. K., 2012. Alleviating monoterpene toxicity using a two-phase extractive fermentation for the bioproduction of jet fuel mixtures in *Saccharomyces cerevisiae*. Biotechnology and bioengineering. 109**,** 2513-22.

Cao, X., Lv, Y. B., Chen, J., Imanaka, T., Wei, L. J., Hua, Q., 2016. Metabolic engineering of oleaginous yeast Yarrowia lipolytica for limonene overproduction. Biotechnology for biofuels. 9**,** 214.

Casey, P. J., 1992. Biochemistry of protein prenylation. Journal of lipid research. 33**,** 1731-40.

Christiano, R., Nagaraj, N., Frohlich, F., Walther, T. C., 2014. Global proteome turnover analyses of the Yeasts *S. cerevisiae* and *S. pombe*. Cell reports. 9**,** 1959-65.

Christianson, T. W., Sikorski, R. S., Dante, M., Shero, J. H., Hieter, P., 1992. Multifunctional yeast high-copy-number shuttle vectors. Gene. 110**,** 119-22.

Dickinson, J. R., Schweizer, M., 2004. Metabolism and molecular physiology of Saccharomyces cerevisiae. CRC press.

Dimster-Denk, D., Rine, J., 1996. Transcriptional regulation of a sterol-biosynthetic enzyme by sterol levels in *Saccharomyces cerevisiae*. Molecular and cellular biology. 16**,** 3981-9.

Dimster-Denk, D., Rine, J., Phillips, J., Scherer, S., Cundiff, P., DeBord, K., Gilliland, D., Hickman, S., Jarvis, A., Tong, L., Ashby, M., 1999. Comprehensive evaluation of isoprenoid biosynthesis regulation in *Saccharomyces cerevisiae* utilizing the Genome Reporter Matrix. Journal of lipid research. 40**,** 850-60.

Entian, K.-D., Kötter, P., 1998. 23 yeast mutant and plasmid collections. Methods in microbiology. 26**,** 431-449.

Farhi, M., Marhevka, E., Masci, T., Marcos, E., Eyal, Y., Ovadis, M., Abeliovich, H., Vainstein, A., 2011. Harnessing yeast subcellular compartments for the production of plant terpenoids. Metabolic engineering. 13**,** 474-481.

Foresti, O., Ruggiano, A., Hannibal-Bach, H. K., Ejsing, C. S., Carvalho, P., 2013. Sterol homeostasis requires regulated degradation of squalene monooxygenase by the ubiquitin ligase Doa10/Teb4. eLife. 2**,** e00953.

Giaever, G., Chu, A. M., Ni, L., Connelly, C., Riles, L., Veronneau, S., Dow, S., Lucau-Danila, A., Anderson, K., Andre, B., Arkin, A. P., Astromoff, A., El-Bakkoury, M., Bangham, R., Benito, R., Brachat, S., Campanaro, S., Curtiss, M., Davis, K., Deutschbauer, A., Entian, K. D., Flaherty, P., Foury, F., Garfinkel, D. J., Gerstein, M., Gotte, D., Guldener, U., Hegemann, J. H., Hempel, S., Herman, Z., Jaramillo, D. F., Kelly, D. E., Kelly, S. L., Kotter, P., LaBonte, D., Lamb, D. C., Lan, N., Liang, H., Liao, H., Liu, L., Luo, C., Lussier, M., Mao, R., Menard, P., Ooi, S. L., Revuelta, J. L., Roberts, C. J., Rose, M., Ross-Macdonald, P., Scherens, B., Schimmack, G., Shafer, B., Shoemaker, D. D., Sookhai-Mahadeo, S., Storms, R. K., Strathern, J. N., Valle, G., Voet, M., Volckaert, G., Wang, C. Y., Ward, T. R., Wilhelmy, J., Winzeler, E. A., Yang, Y., Yen, G., Youngman, E., Yu, K., Bussey, H., Boeke, J. D., Snyder, M., Philippsen, P., Davis, R. W., Johnston, M., 2002. Functional profiling of the Saccharomyces cerevisiae genome. Nature. 418**,** 387-91.

Gietz, R. D., Schiestl, R. H., 2007. High-efficiency yeast transformation using the LiAc/SS carrier DNA/PEG method. Nat. Protocols. 2**,** 31-34.

Green, S. A., Chen, X., Nieuwenhuizen, N. J., Matich, A. J., Wang, M. Y., Bunn, B. J., Yauk, Y. K., Atkinson, R. G., 2012. Identification, functional characterization, and regulation of the enzyme responsible for floral (E)-nerolidol biosynthesis in kiwifruit (*Actinidia chinensis*). Journal of experimental botany. 63**,** 1951-1967.

Hanscho, M., Ruckerbauer, D. E., Chauhan, N., Hofbauer, H. F., Krahulec, S., Nidetzky, B., Kohlwein, S. D., Zanghellini, J., Natter, K., 2012. Nutritional requirements of the BY series of *Saccharomyces cerevisiae* strains for optimum growth. FEMS yeast research. 12**,** 796-808.

Ignea, C., Pontini, M., Maffei, M. E., Makris, A. M., Kampranis, S. C., 2013. Engineering Monoterpene Production in Yeast Using a Synthetic Dominant Negative Geranyl Diphosphate Synthase. ACS synthetic biology.

Jungbluth, M., Renicke, C., Taxis, C., 2010. Targeted protein depletion in *Saccharomyces cerevisiae* by activation of a bidirectional degron. BMC systems biology. 4**,** 176.

Kuranda, K., Francois, J., Palamarczyk, G., 2010. The isoprenoid pathway and transcriptional response to its inhibitors in the yeast *Saccharomyces cerevisiae*. FEMS yeast research. 10**,** 14-27.

Liu, J., Zhang, W., Du, G., Chen, J., Zhou, J., 2013. Overproduction of geraniol by enhanced precursor supply in Saccharomyces cerevisiae. Journal of biotechnology. 168**,** 446-51.

Liu, W., Xu, X., Zhang, R., Cheng, T., Cao, Y., Li, X., Guo, J., Liu, H., Xian, M., 2016. Engineering Escherichia coli for high-yield geraniol production with biotransformation of geranyl acetate to geraniol under fed-batch culture. Biotechnology for biofuels. 9**,** 58.

Livak, K. J., Schmittgen, T. D., 2001. Analysis of relative gene expression data using real-time quantitative PCR and the 2(-Delta Delta C(T)) Method. Methods. 25**,** 402-8.

Mateus, C., Avery, S., 2000. Destabilized green fluorescent protein for monitoring dynamic changes in yeast gene expression with flow cytometry. Yeast (Chichester, England). 16**,** 1313 - 1323.

Meadows, A. L., Hawkins, K. M., Tsegaye, Y., Antipov, E., Kim, Y., Raetz, L., Dahl, R. H., Tai, A., Mahatdejkul-Meadows, T., Xu, L., Zhao, L., Dasika, M. S., Murarka, A., Lenihan, J., Eng, D., Leng, J. S., Liu, C. L., Wenger, J. W., Jiang, H., Chao, L., Westfall, P., Lai, J., Ganesan, S., Jackson, P., Mans, R., Platt, D., Reeves, C. D., Saija, P. R., Wichmann, G., Holmes, V. F., Benjamin, K., Hill, P. W., Gardner, T. S., Tsong, A. E., 2016. Rewriting yeast central carbon metabolism for industrial isoprenoid production. Nature. 537**,** 694-697.

Nielsen, L. K., 2011. Metabolic engineering: from retrofitting to green field. Nature chemical biology. 7**,** 408-9.

Paddon, C. J., Westfall, P. J., Pitera, D. J., Benjamin, K., Fisher, K., McPhee, D., Leavell, M. D., Tai, A., Main, A., Eng, D., Polichuk, D. R., Teoh, K. H., Reed, D. W., Treynor, T., Lenihan, J., Fleck, M., Bajad, S., Dang, G., Dengrove, D., Diola, D., Dorin, G., Ellens, K. W., Fickes, S., Galazzo, J., Gaucher, S. P., Geistlinger, T., Henry, R., Hepp, M., Horning, T., Iqbal, T., Jiang, H., Kizer, L., Lieu, B., Melis, D., Moss, N., Regentin, R., Secrest, S., Tsuruta, H., Vazquez, R., Westblade, L. F., Xu, L., Yu, M., Zhang, Y., Zhao, L., Lievense, J., Covello, P. S., Keasling, J. D., Reiling, K. K., Renninger, N. S., Newman, J. D., 2013. High-level semi-synthetic production of the potent antimalarial artemisinin. Nature. 496**,** 528-32.

Paltauf, F., Kohlwein, S. D., Henry, S. A., 1992. 8 Regulation and Compartmentalization of Lipid Synthesis in Yeast. Cold Spring Harbor Monograph Archive. 21**,** 415-500.

Parks, L. W., Smith, S. J., Crowley, J. H., 1995. Biochemical and physiological effects of sterol alterations in yeast--a review. Lipids. 30**,** 227-30.

Peng, B., Plan, M. R., Carpenter, A., Nielsen, L. K., Vickers, C. E., 2017a. Coupling gene regulatory patterns to bioprocess conditions to optimize synthetic metabolic modules for improved sesquiterpene production in yeast. Biotechnology for biofuels. 10**,** 43.

Peng, B., Plan, M. R., Chrysanthopoulos, P., Hodson, M. P., Nielsen, L. K., Vickers, C. E., 2017b. A squalene synthase protein degradation method for improved sesquiterpene production in *Saccharomyces cerevisiae*. Metabolic engineering. 39**,** 209–219.

Peng, B., Williams, T., Henry, M., Nielsen, L., Vickers, C., 2015. Controlling heterologous gene expression in yeast cell factories on different carbon substrates and across the diauxic shift: a comparison of yeast promoter activities. Microbial cell factories. 14**,** 91.

Poulter, C. D., Rilling, H. C., 1976. Prenyltransferase: the mechanism of the reaction. Biochemistry. 15**,** 1079-83.

Rico, J., Pardo, E., Orejas, M., 2010. Enhanced production of a plant monoterpene by overexpression of the 3-hydroxy-3-methylglutaryl coenzyme A reductase catalytic domain in *Saccharomyces cerevisiae*. Applied and environmental microbiology. 76**,** 6449-54.

Sabri, S., Steen, J. A., Bongers, M., Nielsen, L. K., Vickers, C. E., 2013. Knock-in/Knock-out (KIKO) vectors for rapid integration of large DNA sequences, including whole metabolic pathways, onto the *Escherichia coli* chromosome at well-characterised loci. Microbial cell factories. 12**,** 60.

Saito, A., Rilling, H. C., 1979. Prenyltransferase. Product binding and reaction termination. The Journal of biological chemistry. 254**,** 8511-5.

Sarria, S., Wong, B., Martin, H. G., Keasling, J. D., Peralta-Yahya, P., 2014. Microbial Synthesis of Pinene. ACS synthetic biology.

Scalcinati, G., Knuf, C., Partow, S., Chen, Y., Maury, J., Schalk, M., Daviet, L., Nielsen, J., Siewers, V., 2012. Dynamic control of gene expression in *Saccharomyces cerevisiae* engineered for the production of plant sesquitepene alpha-santalene in a fed-batch mode. Metabolic engineering. 14**,** 91-103.

Servouse, M., Karst, F., 1986. Regulation of early enzymes of ergosterol biosynthesis in *Saccharomyces cerevisiae*. The Biochemical journal. 240**,** 541-7.

Sonderegger, M., Jeppsson, M., Hahn-Hagerdal, B., Sauer, U., 2004. Molecular basis for anaerobic growth of *Saccharomyces cerevisiae* on xylose, investigated by global gene expression and metabolic flux analysis. Applied and environmental microbiology. 70**,** 2307-17.

Stephanopoulos, G., Vallino, J. J., 1991. Network rigidity and metabolic engineering in metabolite overproduction. Science. 252**,** 1675-81.

Suzuki, T., Varshavsky, A., 1999. Degradation signals in the lysine-asparagine sequence space. The EMBO journal. 18**,** 6017-26.

Taxis, C., Stier, G., Spadaccini, R., Knop, M., 2009. Efficient protein depletion by genetically controlled deprotection of a dormant N-degron. Molecular systems biology. 5**,** 267.

Tokuhiro, K., Muramatsu, M., Ohto, C., Kawaguchi, T., Obata, S., Muramoto, N., Hirai, M., Takahashi, H., Kondo, A., Sakuradani, E., Shimizu, S., 2009. Overproduction of geranylgeraniol by metabolically engineered *Saccharomyces cerevisiae*. Applied and environmental microbiology. 75**,** 5536-43.

Vickers, C. E., Behrendorff, J. B., Bongers, M., Brennan, T. C., Bruschi, M., Nielsen, L. K., 2015a. Production of Industrially Relevant Isoprenoid Compounds in Engineered Microbes. Microorganisms in Biorefineries. Springer, pp. 303-334.

Vickers, C. E., Bongers, M., Bydder, S. F., Chrysanthopoulos, P., Hodson, M. P., 2015b. Protocols for the production and analysis of isoprenoids in bacteria and yeast. Springer Protocols Handbooks. Springer, pp. 1-30.

Vickers, C. E., Bongers, M., Liu, Q., Delatte, T., Bouwmeester, H., 2014. Metabolic engineering of volatile isoprenoids in plants and microbes. Plant, cell & environment. 37**,** 1753-75.

Vickers, C. E., Williams, T. C., Peng, B., Cherry, J., 2017. Recent advances in synthetic biology for engineering isoprenoid production in yeast. Current opinion in chemical biology. 40**,** 47-56.

Vik, A., Rine, J., 2001. Upc2p and Ecm22p, dual regulators of sterol biosynthesis in *Saccharomyces cerevisiae*. Molecular and cellular biology. 21**,** 6395-6405.

Willrodt, C., David, C., Cornelissen, S., Buhler, B., Julsing, M. K., Schmid, A., 2014. Engineering the productivity of recombinant *Escherichia coli* for limonene formation from glycerol in minimal media. Biotechnology journal. 9**,** 1000-12.

Xie, W., Ye, L., Lv, X., Xu, H., Yu, H., 2014. Sequential control of biosynthetic pathways for balanced utilization of metabolic intermediates in *Saccharomyces cerevisiae*. Metabolic engineering. 28C**,** 8-18.

Yang, H., Tong, J., Lee, C. W., Ha, S., Eom, S. H., Im, Y. J., 2015. Structural mechanism of ergosterol regulation by fungal sterol transcription factor Upc2. Nature communications. 6**,** 6129.

Zebec, Z., Wilkes, J., Jervis, A. J., Scrutton, N. S., Takano, E., Breitling, R., 2016. Towards synthesis of monoterpenes and derivatives using synthetic biology. Current opinion in chemical biology. 34**,** 37-43.

Zhang, H., Liu, Q., Cao, Y., Feng, X., Zheng, Y., Zou, H., Liu, H., Yang, J., Xian, M., 2014. Microbial production of sabinene--a new terpene-based precursor of advanced biofuel. Microb Cell Fact. 13**,** 20.

Zhao, J., Bao, X., Li, C., Shen, Y., Hou, J., 2016. Improving monoterpene geraniol production through geranyl diphosphate synthesis regulation in Saccharomyces cerevisiae. Applied microbiology and biotechnology. 100**,** 4561-4571.

Zhao, J., Li, C., Zhang, Y., Shen, Y., Hou, J., Bao, X., 2017. Dynamic control of *ERG20* expression combined with minimized endogenous downstream metabolism contributes to the improvement of geraniol production in *Saccharomyces cerevisiae*. Microbial cell factories. 16**,** 17.

Zhuang, X., Engineering novel terpene production platforms in the yeasts *Saccharomyces cerevisiae*. Plant Physiology, Vol. PhD. University of Kentucky, 2013.

Highlights

- Farnesyl pyrophosphate synthase (Erg20p) consumes the monoterpene precursor geranyl pyrophosphate
- N-degron mediated protein degradation and sterol responsive promoters were applied to regulate *ERG20*/Erg20p
- The mevalonate pathway was combinatorially enhanced to facilitate precursor synthesis
- Destabilization of Erg20p effectively improved the production of monoterpenes
- In the final engineered strains, 18 mg L^{-1} linalool or 76 mg L^{-1} limonene were produced